Eigenvalue and Eigenvector Analysis of Stability for a Line of Traffic

By Liang Wang, Berthold K. P. Horn and Gilbert Strang

Many authors have recognized that traffic under the traditional car-following model (CFM) is subject to flow instabilities. A recent model achieves stability using bilateral control (BCM) — by looking both forward and backward [1]. (Looking back may be difficult or distracting for human drivers, but is not a problem for sensors.) We analyze the underlying systems of differential equations by studying their eigenvalues and eigenvectors under various boundary conditions. Simulations further confirm that bilateral control can avoid instabilities and reduce the chance of collisions.

1. Introduction

In the traditional car-following model, the state (including relative position and relative speed) of the current car is controlled to more closely match the state of the leading car [2, 3, 4, 5, 6, 7]. In order to avoid the instability and collision inherent in the car-following system, Horn proposed the bilateral control model [1], in which the state of the current car is controlled to more closely match the average of the states of the leading and following cars. (This is more easily implemented with automatic vehicular control.)

In this paper, we give a theoretical analysis of both the *car-following model* (CFM) and the *bilateral control model* (BCM), by analyzing the eigenvalues and eigenvectors of two ordinary differential equations. Moreover, we give analytical solutions of both models under different boundary conditions, something that does not appear in the original paper[1]. We

Address for correspondence: Prof. Berthold K. P. Horn, Computer Science and Artificial Intelligence Laboratory, Massachusetts Institute of Technology, Cambridge, MA 02139. email: bkph@csail.mit.edu. This work is sponsored by Toyota Motor Corporation (LP-C000765-SR).

DOI: 10.1111/((please add article doi))
STUDIES IN APPLIED MATHEMATICS AA:1–30

prove that bilateral control suppresses traffic instabilities under all of the different boundary conditions — infinite line, circular boundary, fixed-fixed boundaries, free-free boundaries and fixed-free boundaries. In contrast, the car-following model is unstable for any and all of the boundary conditions. For the car-following model under the fixed boundary condition, the corresponding "big matrix" of the ODE system is similar to a *block Jordan form*. There are only two eigenvectors. The "big matrix" is not diagonalizable. We analyze this interesting case and show that its performance is very similar to the case of a circular boundary condition — in which *discrete Fourier transform* (DFT) analysis can be applied. Thus, the overall car-traffic system will become unstable and collisions will occur.

Simulation results confirm the instability of the car-following model. A tiny perturbation in an equilibrium state will soon cause a traffic jam and collisions. Bilateral control can suppress the traffic flow instability and collision very effectively. The traffic system soon returns to an equilibrium state, even in the case that bilateral control is only turned on just before a traffic jam becomes imminent.

2. Related work

A previous attempt at solving traffic flow problems was in the context of a *platoon* [8, 9, 10, 11, 12]. More theoretical analysis of various platoon models was developed in [13, 14]. We should mention that the implementation of bilateral control is very different from that of a platoon. There are significant differences between the two mathematical models:

- All cars in a platoon are led by the first car (for one directional platoon) or both first and last car (for bi-directional platoon). However, bilateral control has no leaders. Every car adjusts its state (position and speed) based on information about the states of its neighbours.
- For platoon models, information about the states of cars in the platoon is transmitted via global communication. For bilateral control, global communication between the cars is not used. The information about the distance and relative speed of the neighbouring cars is measured using sensors on the current car. (Note that bilateral control doesn't exclude the possibility of global communication between the vehicles. Information about neighbouring cars obtained by a communication system can be fused with measurement from the sensors to generate more accurate estimations of the states and to increase the robustness even further [15].)

Bilateral control is more flexible than the platoon model. No other cars are allowed to insert themselves into a platoon, while, other cars can merge in to the traffic flow under bilateral control. Moreover, at least as presently envisaged, the size of each platoon is small (several cars in general), while bilateral control focuses on the whole traffic flow. It seems more practical to use sensor-based control technology (e.g. bilateral control) to solve traffic problem than to build vehicular networking infrastructure.

Mathematically, bilateral control and bi-directional platoon control use the information of the positions of both leading and following cars for control [11, 12]. However, bi-directional platoon control uses the velocity of the first car (or a pre-specified velocity) to adjust the states of *all* cars in the platoon [11, 12]; while bilateral control uses the speed of the *neighbouring* cars to adjust the state of the current car.

Before the invention of bilateral control, there were attempts at using bi-directional information. Nakayama et al. use bi-directional information to improve the traditional optimal velocity (OV) model [16]. Treiber and Helbing use bi-directional information to improve throughput of the traffic system [17]. Horn pointed out that 1) the information from the leading and following cars should contribute equally and 2) adding "dampers" will cause traveling waves to die out [1]. He called this new model *bilateral control* and proved its ability to eliminate the "phantom traffic jams" and "stop-and-go" instabilities (caused by the car-following model).

3. Summary of the car-following and bilateral control models

Let $x_i(t)$ be the position of the $i-$th car, and $v_i(t) = \dot{x}_i(t)$ be its velocity[1]. The pair $\{x_i(t), v_i(t)\}$ gives the state of the $i-$th car, which is adjusted through the acceleration $a_i(t) = \ddot{x}_i(t)$ commanded by the control system. For the car-following model[2] (CFM),

$$a_i = k_d(x_{i-1} - x_i - s) + k_v(v_{i-1} - v_i) \tag{1}$$

where s is known as the *safe distance*, $k_d > 0$, and $k_v > 0$ are the proportional and derivative gains respectively. In this model, control of car i is based *only* on the relative position and relative velocity of car $i-1$

[1]Note that x_{i-1} and x_i denote the position of the leading and current cars. The positive direction is chosen as the direction in which cars are moving, thus, $x_{i-1} - x_i > 0$ (see Figure 1).

[2]Here we only consider the case where the velocity of the cars are all between zero and the speed limit of the highway. Otherwise, the difference between the car's current velocity and a desired velocity, denoted by $v_i - v_{\text{des}}$, should be added as a control input [1].

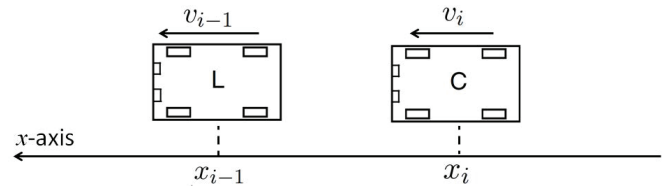

(a) Car-following model

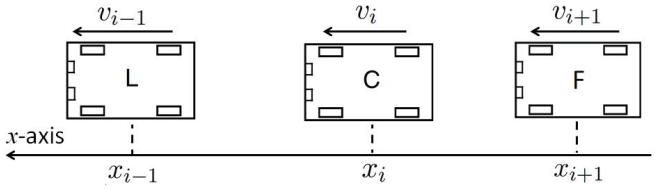

(b) Bilateral control model

Figure 1: Illustration of the car-following model and bilateral control model. The blocks with "L", "C" and "F" denote the leading car, current car and following car. (a) Car-following control is based *only* on the state of the leading car "L". (b) Bilateral control uses the states of *both* leading car "L" and following car "F".

immediately ahead. For the bilateral control model (BCM),

$$a_i = \frac{1}{2}k_d\big((x_{i-1} - x_i) - (x_i - x_{i+1})\big) + \frac{1}{2}k_v\big((v_{i-1} - v_i) - (v_i - v_{i+1})\big) \quad (2)$$

Now the control of car i is based on the relative positions and relative velocities of *both* car $i-1$ ahead and car $i+1$ behind. Figure 1 shows the two models.

In the ideal case, all the cars are spaced the safe distance s apart and move at the same speed v_0. In this case, all the accelerations a_i in eqs. (1) and (2) are zero, and the traffic continues in the *equilibrium state*. The important question then is whether this equilibrium is stable, meta-stable, or unstable. If there is a small perturbation in $x_i(t)$ or $v_i(t)$, will the traffic system return to the equilibrium state or will there be increasing departures from the equilibrium, which ultimately lead to a traffic jam? To answer this question, we will analyse eqs. (1) and (2).

4. The eigenvalue-and-eigenvector based analysis

For convenience, we change variables:

$$y_i(t) = x_i(t) + i \times s - v_0 t \quad (3)$$

Then eqs. (1) and (2) can be written in the form:

$$\text{CFM:} \qquad \ddot{y}_i + k_v \dot{y}_i + k_d y_i = k_v \dot{y}_{i-1} + k_d y_{i-1} \tag{4}$$

$$\text{BCM:} \qquad \ddot{y}_i + k_v \dot{y}_i + k_d y_i = k_v \frac{1}{2}\left(\dot{y}_{i-1} + \dot{y}_{i+1}\right) + k_d \frac{1}{2}\left(y_{i-1} + y_{i+1}\right) \tag{5}$$

Now $\{y_i(t), \dot{y}_i(t)\}$ are the state of the $i-$th car in the relative reference system (relative position and relative speed). Note that the left sides of eqs. (4) and (5) are the same, and correspond to a spring-damper-mass system. The right sides of eqs. (4) and (5) describe the external input to that spring-damper-mass system. The external inputs of the system can be imagined as a "moving" wall (see Fig. 2b). For the car-following model, the state of the "moving" wall is chosen as the state of the leading car. For bilateral control model, the state of the "moving" wall is chosen as the *average* of the states of the leading and following cars.

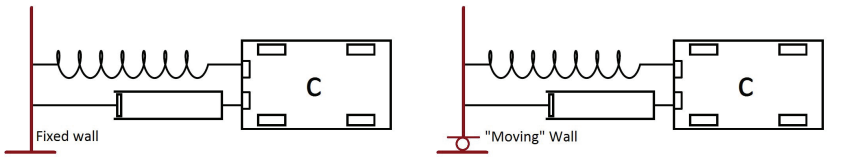

(a) Fixed wall boundary (b) "Moving" wall boundary

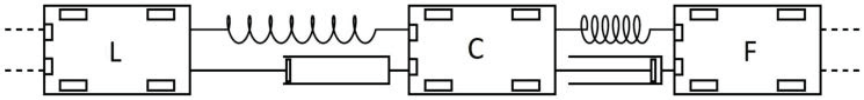

(c) Physical model of the bilateral control system

Figure 2: The second order ODEs (4) and (5) describe a spring-damper-mass system. The right side of eqs. (4) and (5) are the external inputs. (a) If the right side of eqs. (4) or (5) is zero, then the system is attached to a fixed wall. (b) The external inputs of the system can be imagined as a "moving" wall. For the car-following model, the state of the "moving" wall is chosen as the state of the leading car. For bilateral control model, the state of the "moving" wall is chosen as the *average* of the states of the leading and following cars. (c) Bilateral control obeys *Newton's third law*. All the spring-damper-mass modules can be cascaded physically as a large system. That is not the case for the car-following model.

First, note that the car-following model does not correspond directly to a real mechanical system, because it does not obey *Newton's third law*. The state of the leading car acts on the effective spring and damper connected to the $i-$th car, while the car $i-1$ does *not* react to changes from the following driver i. It is as if a "buffer" device was inserted that replicates the position of the leading car. The spring and damper would be attached to this "buffer", not the leading car directly. The bilateral control model on the other hand *does* correspond to a real physical system

and obeys Newton's third law. This makes it possible to employ physical intuition for BCM. For instance, the spring-damper-mass modules can be cascaded physically as one large system (see Fig. 2c). Intuitively, the waves caused by perturbation of one of the masses will travel in two opposite directions, and be damped as they travel.

4.1. The "big ODE system"

For easy analysis, we rewrite the second order ODE as two first order ODEs. Eqs. (4) and (5) can be written as:

$$\text{CFM:} \qquad \frac{d}{dt}Y_i = NY_{i-1} + MY_i \tag{6}$$

$$\text{BCM:} \qquad \frac{d}{dt}Y_i = \frac{1}{2}NY_{i-1} + MY_i + \frac{1}{2}NY_{i+1} \tag{7}$$

where

$$Y_i = \begin{pmatrix} y_i \\ \dot{y}_i \end{pmatrix}, \qquad N = \begin{pmatrix} 0 & 0 \\ k_d & k_v \end{pmatrix}, \qquad M = \begin{pmatrix} 0 & 1 \\ -k_d & -k_v \end{pmatrix}$$

Let $\mathbf{Y} = (\cdots, Y_{i-1}^T, Y_i^T, Y_{i+1}^T, \cdots)^T$ be the *state vector* containing the states of all the cars in the traffic system. From eqs. (6) and (7), we can build two *big ODE systems*:

$$\text{(CFM)} \quad \frac{d}{dt}\mathbf{Y} = \mathbf{A}\mathbf{Y} \qquad \text{and} \qquad \text{(BCM)} \quad \frac{d}{dt}\mathbf{Y} = \mathbf{B}\mathbf{Y} \tag{8}$$

$\mathbf{A}$ and $\mathbf{B}$ are both *block-constant-diagonal* (or *block-Toeplitz*) matrices:

$$\mathbf{A} = \begin{pmatrix} \ddots & & & & \\ \ddots & M & & & \\ & N & M & & \\ & & N & M & \\ & & & \ddots & \ddots \end{pmatrix}, \mathbf{B} = \begin{pmatrix} \ddots & \ddots & & & \\ \ddots & M & N/2 & & \\ & N/2 & M & N/2 & \\ & & N/2 & M & \ddots \\ & & & \ddots & \ddots \end{pmatrix}$$

The solutions are[3]:

$$\text{(CFM)} \quad \mathbf{Y}(t) = e^{t\mathbf{A}}\mathbf{Y}(0) \qquad \text{and} \qquad \text{(BCM)} \quad \mathbf{Y}(t) = e^{t\mathbf{B}}\mathbf{Y}(0) \tag{9}$$

where $\mathbf{Y}(0)$ is the *initial state* of the traffic system. The traffic's stability can be determined by analyzing the eigenvalues of the "big matrices" $\mathbf{A}$ and $\mathbf{B}$ [18].

---

[3]For a *doubly infinite Toeplitz matrix* $\mathbf{A}$, we can define $e^{t\mathbf{A}}\mathbf{Y}(0) = S\big(e^{\lambda(\omega)t}S^{-1}\mathbf{Y}(0)\big)$. Here, $S^{-1}\mathbf{Y}(0)$ denotes the *discrete-time Fourier transform* (DTFT) of $\mathbf{Y}(0)$, and $S(f(\omega))$ denotes the inverse DTFT of $f(\omega)$. And $\lambda(\omega)$ — called the eigenvalue (function) of $\mathbf{A}$ — is the DTFT of one row of $\mathbf{A}$.

4.2. Eigenvalues and eigenvectors of the "Big Matrix"

First, if M and N were scalars (rather than 2×2 matrices), then $\mathbf{A}$ and $\mathbf{B}$ would both be *Toeplitz matrices* (i.e. *linear convolution systems*). The *discrete-time Fourier transform* (DTFT) will solve the eigenvalue-and-eigenvector problem [19]. The eigenvector $u(\omega)$ should be of the form:

$$u(\omega) = (\cdots, w^{l-1}, w^l, w^{l+1}, \cdots)^T$$

where $w = w(\omega) = e^{-j\omega}$, and the corresponding eigenvalue (for CFM) would be:

$$\lambda(\omega) = M + Nw \tag{10}$$

In our case, M and N are both 2×2 matrices. One more step is needed. The eigenvector $U(\omega)$ is the *Kronecker tensor product* of $u(\omega)$ and a 2×1 vector $p(\omega) = (a(\omega), b(\omega))^T$:

$$\begin{aligned} U(\omega) &= u(\omega) \otimes p(\omega) \qquad (11)\\ &= (\cdots, a(\omega)w^{l-1}, b(\omega)w^{l-1}, a(\omega)w^l, b(\omega)w^l, a(\omega)w^{l+1}, b(\omega)w^{l+1}, \cdots)^T \end{aligned}$$

where $w = e^{-j\omega}$ as above. For CFM, the eigenvalue $\lambda(\omega)$ corresponding to $U(\omega)$ can be found by solving

$$\lambda(\omega)p(\omega) = Mp(\omega) + w(\omega)Np(\omega)$$

That is, $\lambda(\omega)$ and $p(\omega)$ are the eigenvalue and eigenvector of the 2×2 matrix $M + w(\omega)N$. The corresponding characteristic equation is:

$$\lambda^2(\omega) + \big(1 - w(\omega)\big)k_v\lambda(\omega) + \big(1 - w(\omega)\big)k_d = 0 \tag{12}$$

Note that the sum of the real parts of the two eigenvalues is smaller or equal to zero. Thus, the real part of one of the eigenvalues must be smaller or equal to zero. It's not as easy to determine the sign of the real part of the other eigenvalue. However, the result is as following

- the real part of the other root of eq. (12) is greater than zero, except in the extreme case when $k_d = 0$.

One way of seeing this conclusion is to consider the case that ω is pretty small, such that $1 - e^{-j\omega} \approx j\omega$. Then eq. (12) can be approximated by

$$\lambda^2(\omega) + j\omega k_v\lambda(\omega) + j\omega k_d = 0$$

The real part of the two roots are

$$\pm\frac{\sqrt{2}}{4}\sqrt{-\omega^2k_v^2 + \sqrt{(\omega^2k_v^2)^2 + 16\omega^2k_d^2}}$$

The real part of both roots is zero if and only if $k_d = 0$. Otherwise, the real part of one root must be positive. In Appendix A, we give a rigorous proof of the following result:

- the eigenvalues have non-positive real part for the car-following model only in the extreme case $k_d = 0$. Then the control systems ignores the distance to the leading car and uses only the relative speed of the leading car.

However, this special control stratagem is pretty dangerous — there is no assurance that the trajectory of a car won't "cross over" those of the cars ahead and behind (after all, no attention is paid to the relative positions). Thus this method cannot be used. Even if k_d is small, e.g. $k_v/k_d = 100$, some eigenvalues will have positive real part and traffic instabilities will occur.

For BCM, the eigenvectors are also of the form $U(\omega) = u(\omega) \otimes p(\omega)$, however, the eigenvalues are found by solving:

$$\begin{aligned}\lambda(\omega)p(\omega) &= Mp(\omega) + \frac{1}{2}(e^{-j\omega} + e^{j\omega})Np(\omega) \\ &= \big(M + N\cos(\omega)\big)p(\omega)\end{aligned}$$

Similarly, $\lambda(\omega)$ and $p(\omega)$ are the eigenvalue and eigenvector of the 2×2 matrix $M + N\cos(\omega)$. The corresponding characteristic equation is:

$$\lambda^2(\omega) + \big(1 - \cos(\omega)\big)k_v\lambda(\omega) + \big(1 - \cos(\omega)\big)k_d = 0 \tag{13}$$

The sum of these two eigenvalues is $-(1-\cos(\omega))k_v \leq 0$, and the product of these two eigenvalues is $(1 - \cos(\omega))k_d \geq 0$. Thus, the real parts of both eigenvalues are smaller than or equal to zero. The only case where the eigenvalue is zero is when $\omega = 0$, which corresponds to the *equilibrium state* where the cars are spaced equally and are moving at the same speed. The car-state mode corresponding to other eigenvectors $U(\omega)$ (with $\omega \neq 0$) will decay to zero. Thus, the traffic system goes to the equilibrium state from an arbitrary initial state when using bilateral control. That is, bilateral control can suppress traffic flow instabilities.

5. Boundary conditions

In section 4, we haven given an eigenvalue-and-eigenvector analysis of both car-following and bilateral control models, and show the bilateral control's advantage of suppressing traffic flow instabilities. For easy analysis, we didn't yet consider boundary conditions. In the above, both matrices **A** and **B** were doubly infinite. We should also consider the case when the total number of cars is finite, and this means that we need to

consider boundary conditions on the line of traffic. Next, we analyze both models under various boundary conditions.

5.1. Circular boundary condition

Suppose that there are totally K cars moving on a circle. That is, car K is immediately ahead of car 1. Now, both $\mathbf{A}$ and $\mathbf{B}$ become finite $(2K \times 2K)$ block circulant matrices:

$$\mathbf{A} = \begin{pmatrix} M & & & N \\ N & M & & \\ & \ddots & \ddots & \\ & & N & M \end{pmatrix}, \mathbf{B} = \begin{pmatrix} M & N/2 & & N/2 \\ N/2 & M & \ddots & \\ & \ddots & \ddots & N/2 \\ N/2 & & N/2 & M \end{pmatrix}$$

The Fourier-transform approach used in Section 4 still works, only now we use the *Discrete Fourier Transform* (DFT). That is, ω is sampled as $\big(0, \Delta\omega, 2\Delta\omega, \cdots, k\Delta\omega, \cdots, (K-1)\Delta\omega\big)^T$ — K equally-spaced points with $K\Delta\omega = 2\pi$. Now $u(\omega)$ becomes a finite vector u_k with K entries:

$$u_k = (1, w_k, w_k^2, \cdots, w_k^l, w_k^{l+1}, \cdots, w_k^{K-1})^T$$

where $w_k = e^{-2\pi jk/K}$ (for $k = 0, 1, 2, \cdots, K-1$). The eigenvector U_k is the *Kronecker tensor product* of u_k and a 2×1 vector $p_k = (a_k, b_k)^T$:

$$\begin{aligned} U_k &= u_k \otimes p_k \\ &= (a_k, b_k, w_k a_k, w_k b_k, \cdots, w_k^l a_k, w_k^l b_k, \cdots, w_k^{K-1} a_k, w_k^{K-1} b_k)^T \end{aligned} \tag{14}$$

For CFM, the eigenvalue equation $\lambda_k p_k = (M + w_k N) p_k$ leads to

$$\lambda_k^2 + (1 - w_k) k_v \lambda_k + (1 - w_k) k_d = 0. \tag{15}$$

In Appendix A, we will show that the condition for all $\Re\{\lambda_k\} \leq 0$ is:

$$\frac{k_v^2}{k_d} \geq \frac{1}{2}\left(\frac{1}{\sin^2(\pi/K)} - 1\right) \approx \frac{K^2}{2\pi^2}$$

In practice it is not possible to satisfy this condition. For instance, in a small traffic system containing just 10 cars, if $k_v = 0.2$, then k_d must be less than 0.008 (which is too small to keep safe distance). Figure 3 shows a simulation by MATLAB.

In bilateral control, λ_k and p_k are the eigenvalue and eigenvector of the 2×2 matrix $M + (1 - \cos(2\pi k/K))N$. The eigenvalue λ_k comes from

$$\lambda_k^2 + \big(1 - \cos(2\pi k/K)\big) k_v \lambda_k + \big(1 - \cos(2\pi k/K)\big) k_d = 0 \tag{16}$$

Still all $\lambda_k \leq 0$, with $\lambda_k = 0$ only when $k = 0$ (corresponding to the equilibrium state). The traffic goes to the equilibrium state from arbitrary initial state when using bilateral control.

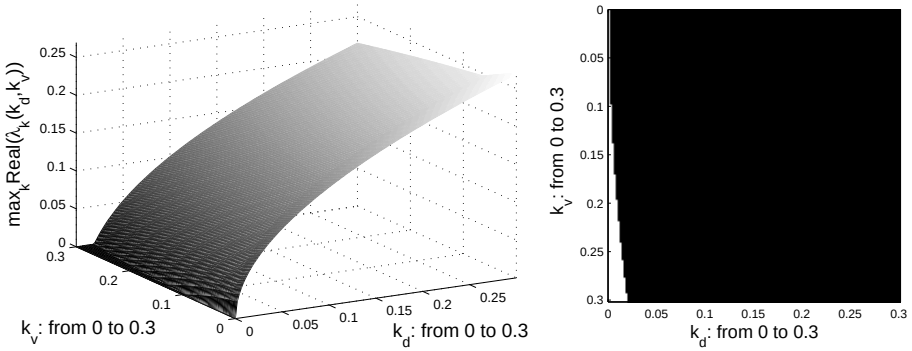

(a) Small system ($K = 10$) (b) Support set of (a)

Figure 3: The maximum real part of the eigenvalues for the car-following model, denoted by $\lambda_{\max} = \max_k\{\text{Real}(\lambda_k(k_d, k_v))\}$, under the circular boundary condition. Both k_d and k_v are in the range from 0 to 0.3. Even when K is small enough, e.g. $K = 10$, the region such that $\lambda_{\max} = 0$ is still pretty small (the "white region" in (b)). The choice of k_d in the "white region" of (b) is too close to zero to be useful in real applications.

5.2. Other boundary conditions for the bilateral control model

For other boundary conditions, e.g. fixed-fixed, free-free and fixed-free, the eigenvalue decomposition analysis still works to analyze the bilateral control model under these three boundary conditions. Suppose that there are $K + 2$ cars in the traffic system. The state of the first car, i.e. $\{y_0, \dot{y}_0\}$, and the state of the last car, i.e. $\{y_{K+1}, \dot{y}_{K+1}\}$, provide the boundary condition. The states of the other K cars form the *state vector* $\mathbf{Y} = (y_1, \dot{y}_1, y_2, \dot{y}_2, \cdots, y_i, \dot{y}_i, \cdots, y_K, \dot{y}_K)^T$. The form of $\mathbf{B}$ depends on the particular type of boundary conditions.

5.2.1. Fixed-fixed boundary. Suppose that car 0 and car $K + 1$ are moving at the (same) constant speed (or both fixed in the relative reference system), that is, $y_0 = y_{K+1} = 0$ and $\dot{y}_0 = \dot{y}_{K+1} = 0$. Then, the matrix $\mathbf{B}$ is

$$\mathbf{B} = \begin{pmatrix} M & N/2 & & \\ N/2 & M & \ddots & \\ & \ddots & \ddots & N/2 \\ & & N/2 & M \end{pmatrix}$$

The vector u_k is exactly the $k-$th basis vector of the $K-$point *Discrete Sine Transform* (DST):

$$u_k = (\sin(kh), \sin(2kh), \cdots, \sin(Kkh))^T$$

with $k = 1, 2, \cdots, K$ and $h = \pi/(K+1)$. The eigenvector $U_k = u_k \otimes p_k$ is the *Kronecker tensor product* of u_k and a 2×1 vector $p_k = (a_k, b_k)^T$. The eigenvalue equation $\lambda_k p_k = (M + N\cos(kh))\, p_k$ leads to

$$\lambda_k^2 + (1 - \cos(kh))\, k_v \lambda_k + (1 - \cos(kh))\, k_d = 0 \tag{17}$$

Now, all the eigenvalues are with negative real part. Thus, the final state is $\mathbf{Y}(\infty) = \mathbf{0}$, that is, a special case of the equilibrium state. Note that the first and last cars are fixed, thus, the total length of the traffic system does not change. The final speed of the traffic system is the same as the speed of the first car (and the last car).

5.2.2. Free-free boundary. Suppose that the state of the boundary car 0 is the same as the state of the car 1 behind (in the relative reference), i.e., $y_0 = y_1$ and $\dot{y}_0 = \dot{y}_1$, moreover, the state of the boundary car $K+1$ is also the same as the state of the car K ahead, i.e., $y_{K+1} = y_K$ and $\dot{y}_{K+1} = \dot{y}_K$. Note that the states of the boundaries (cars 0 and car $K+1$) are changing to match the states of their neighbors, rather than fixed. Now, the matrix $\mathbf{B}$ is

$$\mathbf{B} = \begin{pmatrix} M_1 & N/2 & & \\ N/2 & M & \ddots & \\ & \ddots & \ddots & N/2 \\ & & N/2 & M_1 \end{pmatrix}$$

where

$$M_1 = \begin{pmatrix} 0 & 1 \\ -k_d/2 & -k_v/2 \end{pmatrix}$$

The vector u_k is in the $K-$point *Discrete Cosine Transform* (DCT) basis:

$$u_k = (\cos((1-1/2)kh), \cos((2-1/2)kh), \cdots, \cos((K-1/2)kh))^T$$

with $k = 0, 1, 2, \cdots, K-1$ and $h = \pi/K$. The eigenvector $U_k = u_k \otimes p_k$ is the *Kronecker tensor product* of u_k and a 2×1 vector $p_k = (a_k, b_k)^T$. The eigenvalue equation $\lambda_k p_k = (M + N\cos(kh))\, p_k$ leads to

$$\lambda_k^2 + (1 - \cos(kh))\, k_v \lambda_k + (1 - \cos(kh))\, k_d = 0 \tag{18}$$

The real part of λ_k is less than zero for $k = 1, \cdots, K-1$. The only case that $\lambda_k = 0$ is $k = 0$. The corresponding state is $\mathbf{Y}(t) = (a_0 + b_0 t, b_0, a_0 + b_0 t, b_0, \cdots, a_0 + b_0 t, b_0)^T$, when all the relative positions (and also relative speeds) are shifted by the same amount. We can choose new relative position and speed such that $\mathbf{Y}(t) = \mathbf{0}$. Thus, free-free boundaries model the traffic system from one equilibrium state to another equilibrium state by bilateral control, during which the relative speed and the space between

the successive cars can be adjusted to match the demanded values. This illustrates the flexibility of BCM.

5.2.3. Fixed-free boundary. Another interesting boundary condition is fixed-free. Car 0 (one boundary) is moving at a constant speed, i.e. $y_0 = \dot{y}_0 = 0$. The state of car $K+1$ (the other boundary) matches the state of its neighboring car K, that is, $y_{K+1} = y_K$ and $\dot{y}_{K+1} = \dot{y}_K$. Now, the matrix $\mathbf{B}$ is

$$\mathbf{B} = \begin{pmatrix} M & N/2 & & \\ N/2 & M & \ddots & \\ & \ddots & \ddots & N/2 \\ & & N/2 & M_1 \end{pmatrix}$$

And the vector u_k is equally-spaced sampling K points of $\sin((2k-1)\omega)$ in the range of $0 < \omega < \pi/2$

$$u_k = \left(\sin\left((k-1/2)h\right), \sin\left((k-1/2)2h\right), \cdots, \sin\left((k-1/2)Kh\right)\right)^T$$

with $k = 1, 2, \cdots, K$ and $h = \pi/(K+1/2)$. The eigenvector $U_k = u_k \otimes p_k$ is the *Kronecker tensor product* of u_k and a 2×1 vector $p_k = (a_k, b_k)^T$. The eigenvalue equation $\lambda_k p_k = (M + N\cos\left((k-1/2)h\right)) p_k$ leads to

$$\lambda_k^2 + \left(1 - \cos\left((k-1/2)h\right)\right) k_v \lambda_k + \left(1 - \cos\left((k-1/2)h\right)\right) k_d = 0 \quad (19)$$

Now, the real part of λ_k is negative for all $k = 1, 2, \cdots, K$. Thus, the final state is $\mathbf{Y}(\infty) = \mathbf{0}$. All the cars are equally spaced and move at the same speed. The state of the first car is fixed (used as the reference). The last car's state matches its leading car (this is what the car-following model tries to implement). The final speed of the traffic system is the same as the speed of the first car in this case. Moreover, the total length of the traffic system can be changing during the process of going to the equilibrium state (which is different from the case of the fixed-fixed boundaries)

Figure 4 shows the numerical results of the real part of the eigenvalues $\{\lambda_k\}$ for the bilateral control model under the various four boundary conditions: circular, fixed-fixed, free-free and fixed-free. The parameters are set as $k_d = k_v = 0.2$ and $K = 100$. All the eigenvalues are with non-positive real part[4]. Comparing eq. (13) with eqs. (16), (17), (18) and (19), respectively, we can see that the eigenvalues of the bilateral control model under different boundary conditions (circular, fixed-fixed, free-free and fixed-free) are exactly the equally spaced sampling results of the (continuous) eigenvalues in the infinite boundary condition (that

[4]The eigenvalues calculated by MATLAB command "eig( )" are sorted on their norm. Then, we resort the eigenvalues by their real part.

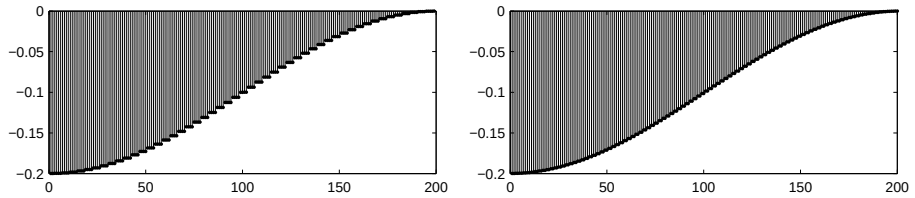

(a) Circular boundary condition

(b) Fixed-fixed boundary condition

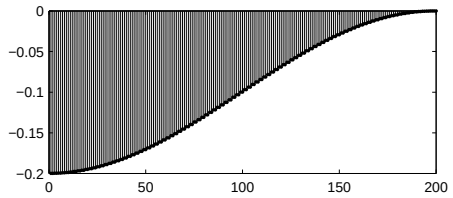

(c) Free-free boundary condition

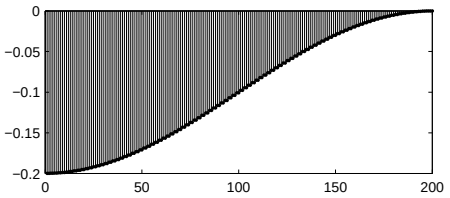

(d) Fixed-free boundary condition

Figure 4: The real-part of the eigenvalues of the bilateral control model under various boundary conditions. The parameters are chosen as $k_d = k_v = 0.2$ and $K = 100$. All the eigenvalues have non-positive real part. The labels under the horizontal axis are the indices of the eigenvalues.

is, it is not necessary to consider the boundary condition), with the step size $\Delta\omega$ chosen as $2\pi/K$, $\pi/(K+1)$, π/K and $\pi/(K+1/2)$, respectively. The bilateral control model is stable under the infinity boundary condition, thus, it will also be stable under these four different finite boundary conditions.

5.3. Other boundary conditions for the car-following model

From the analysis in section 5.2, we can see that there are two steps to find the eigenvalues and eigenvectors of the "big matrix" $\mathbf{A}$ and $\mathbf{B}$:

1. find the eigenvector u_k of the matrix generated by replacing the "blocks" M and N in the "big matrix" with two scalars.
2. eigenvector U_k is the Kronecker tensor product of u_k and a 2×1 vector p_k which is an eigenvector of a 2×2 matrix.

In the case of bilateral control model, if the "blocks" M and N are treated as two scalars, then $\mathbf{B}$ will become a symmetric matrix for all of the three special boundary conditions (fixed-fixed, free-free and fixed-free). Thus, $\mathbf{B}$ is diagonalizable [18], that is, there are enough eigenvectors to span the whole space.

However, for the car-following model, the eigenvalue decomposition analysis doesn't work for other boundary conditions. The "big matrix" $\mathbf{A}$ can not be diagonalized when M and N are treated as scalars. For

instance, in the fixed boundary condition[5], the "big matrix" $\mathbf{A}$ is

$$\mathbf{A} = \begin{pmatrix} M & & & & \\ N & M & & & \\ & N & M & & \\ & & \ddots & \ddots & \\ & & & N & M \end{pmatrix}$$

If M and N are treated as scalars, then the matrix $\mathbf{A}$ will be *similar* to a *Jordan block*. There are two matrices D and J:

$$D = \begin{pmatrix} 1 & & & & \\ & N & & & \\ & & N^2 & & \\ & & & \ddots & \\ & & & & N^{K-1} \end{pmatrix}, \; J = \begin{pmatrix} M & & & & \\ 1 & M & & & \\ & 1 & M & & \\ & & \ddots & \ddots & \\ & & & 1 & M \end{pmatrix}$$

such that

$$D\mathbf{A}D^{-1} = J \tag{20}$$

Note that J is the transpose of a $K \times K$ Jordan block. Thus, there are K repeated eigenvalues $\lambda_0 = M$, but only one eigenvector

$$u_0 = (0, 0, \cdots, 0, 0, 1)^T$$

In this case[6], the states of the cars can be calculated by:

$$\mathbf{Y}(t) = e^{t\mathbf{A}}\mathbf{Y}(0) = D^{-1}e^{tJ}D\mathbf{Y}(0) \tag{21}$$

where $e^{tJ} = e^{t\lambda_0}L$, and L is a *lower triangular Toeplitz* matrix:

$$L = \begin{pmatrix} 1 & & & & & \\ t & 1 & & & & \\ \frac{t^2}{2} & t & 1 & & & \\ \frac{t^3}{3!} & \frac{t^2}{2} & t & 1 & & \\ \vdots & \ddots & \ddots & \ddots & \ddots & \\ \frac{t^{K-1}}{(K-1)!} & \cdots & \frac{t^3}{3!} & \frac{t^2}{2} & t & 1 \end{pmatrix} \tag{22}$$

The entries in the first column of L are exactly the first K terms of the Taylor expansion of e^t. If $\lambda_0 = M$ is negative, then all the entries in the matrix e^{tJ} (and the sum of each row) go to zero when t is sufficiently large. However, when K is infinite, the sum of each row becomes $e^{t(\lambda_0+1)}$,

[5]Note that the boundary condition for the car-following model is just the state of the first car, rather than the states of both of the first and last cars (as used in the BCM).

[6]M is treated as a scalar temporarily, we will give the solution when M is a 2×2 matrix later.

which could go to infinity even if λ_0 is negative. Moreover, when K is infinite, the eigenvalue of the matrix e^{tJ} becomes $e^{t(\lambda_0+e^{-j\omega})}$. The stability depends on the value of $\lambda_0 + e^{-j\omega}$, rather than λ_0 itself.

When M and N are both 2×2 matrices, the two eigenvalues λ_1 and λ_2 of M can be found from

$$Mp_k = \lambda_k M, \qquad (k = 1, 2). \tag{23}$$

The corresponding characteristic equation is:

$$\lambda_k^2 + k_v \lambda_k + k_d = 0 \tag{24}$$

The two roots λ_1 and λ_2 both have negative real parts. Note that λ_1 and λ_2 are the two (K repeated) eigenvalues of the "big matrix" $\mathbf{A}$, and the corresponding two eigenvectors are $U_k = u_0 \otimes p_k$ (with $k = 1, 2$). However, as mentioned above, having negative real part for both λ_1 and λ_2 doesn't imply that the traffic system is stable. While the size of the matrix $\mathbf{A}$ is $2K \times 2K$. Eigenvalue decomposition analysis doesn't work here. Actually, $\mathbf{A}$ is similar to a *block-Jordan Form* $\mathbf{J}$, i.e. $\mathbf{A} = \mathbf{EJE}^{-1}$, where

$$\mathbf{J} = \begin{pmatrix} J_1 & \\ & J_2 \end{pmatrix}$$

and J_1 and J_2 are both $K \times K$ *Jordan blocks*:

$$J_1 = \begin{pmatrix} \lambda_1 & & & & \\ 1 & \lambda_1 & & & \\ & 1 & \lambda_1 & & \\ & & \ddots & \ddots & \\ & & & 1 & \lambda_1 \end{pmatrix}, \quad J_2 = \begin{pmatrix} \lambda_2 & & & & \\ 1 & \lambda_2 & & & \\ & 1 & \lambda_2 & & \\ & & \ddots & \ddots & \\ & & & 1 & \lambda_2 \end{pmatrix}$$

In Appendix B, we give the proof and the detailed form of the $2K \times 2K$ invertible matrix $\mathbf{E}$. The analytical solution of the car-following model under the fixed boundary condition is:

$$\mathbf{Y}(t) = e^{t\mathbf{A}}\mathbf{Y}(0) = \mathbf{E}e^{t\mathbf{J}}\mathbf{E}^{-1}\mathbf{Y}(0) = \mathbf{E}\begin{pmatrix} e^{tJ_1} & \\ & e^{tJ_2} \end{pmatrix}\mathbf{E}^{-1}\mathbf{Y}(0) \tag{25}$$

where $e^{tJ_i} = e^{t\lambda_i}L$ (for $i = 1, 2$), and L is the lower triangular matrix in (22). Even though both λ_1 and λ_2 have negative real parts, these matrices grow large in finite time before decaying to zero (see Figure 6). Traffic instability will still occur.

Figure 5 shows the real parts of the eigenvalues $\{\lambda_k\}$ of the car-following model under the circular and fixed boundaries (by MATLAB). The parameters are set as $k_d = k_v = 0.2$ and $K = 100$. Note that, although there are theoretically only 2 eigenvalues in the fixed boundary

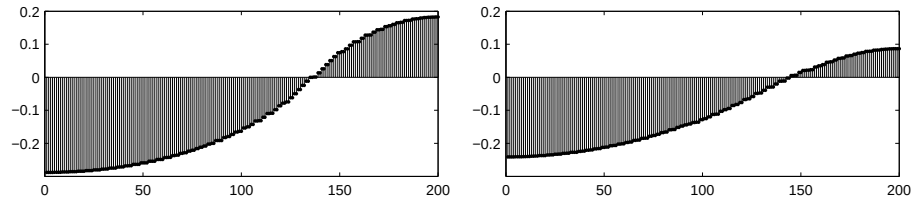

(a) Circular boundary condition (b) Fixed boundary condition

Figure 5: The numerical results of the real-part of the eigenvalues of the car-following model under various boundary conditions ($k_d = k_v = 0.2$ and $K = 100$). Some of the "eigenvalues" (obtained by the numerical algorithm) have positive real parts.

case, the numerical algorithm gives some "eigenvalues" with positive real part[7].

Figure 6 shows the norm of $e^{t\mathbf{A}}$ — the maximum *singular value* of $e^{t\mathbf{A}}$ — for circular and fixed boundaries. Note that the vertical axis uses the logarithmic coordinates. In the circular boundary condition, $||e^{t\mathbf{A}}||$ increases exponentially with time t. In the fixed boundary condition, $||e^{t\mathbf{A}}||$ increases approximately exponentially when t is not large, e.g. $t < 250$, and decays only when t is large enough, e.g. $t > 900$. In the fixed boundary condition, $||e^{t\mathbf{A}}||$ will decay finally because both of the eigenvalues have negative real part, However, $||e^{t\mathbf{A}}||$ becomes very large (more than 10^{20}) before decaying. Thus traffic jams will still occur.

Here we should mention that a modification of CFM that is closer to human driver's actual behavior is known as "constant time headway" control, in which the safe distance s is chosen adaptively according to the car's speed, i.e. $s_i = v_i T$ (with constant T), rather than a fixed headway distance s. The eigenvalue-eigenvector analysis used above can be used to analyze this new model as well. The details are summarized in Appendix C. Comparing this to the simple CFM in (1), the stability condition (A.7) is relaxed as shown in (C.21) when the adaptive safe distance is used. However, condition (C.21) provides a critical limitation on the traffic throughput (see eq. (C.22)). It corresponds to our experience that at low densities there may be few problems, but that at high densities flow instabilities ("phantom traffic jams") will occur.

[7]Note that the numerical algorithm is not guaranteed to find the correct eigenvalues. Nevertheless, the numerical solutions for some of the eigenvalues predict the performance of the system. Some "eigenvalues" estimated by the numerical algorithm have positive real parts (as shown in Fig. 5b). Thus, the corresponding components of a perturbation will be amplified very quickly when they are multiplied by the matrix $\mathbf{A}$ for finite times. Thus, car-following control with fixed boundary conditions will also lead to traffic jams (or result in collisions).

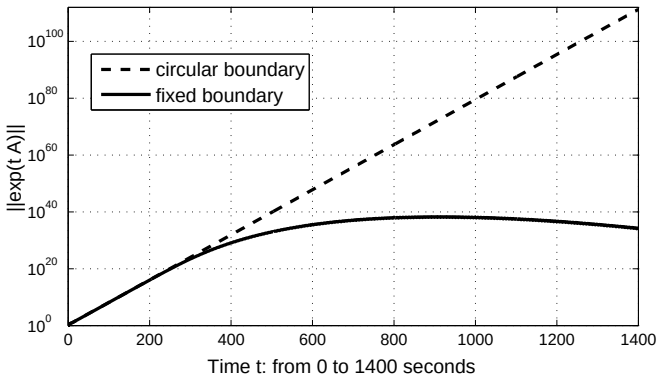

Figure 6: The norm of $e^{t\mathbf{A}}$ in the circular boundary (dash line) and fixed boundary (solid curve). In the circular boundary, $||e^{t\mathbf{A}}||$ increases exponentially with time t. In the fixed boundary, $||e^{t\mathbf{A}}||$ increases approximately exponentially at the beginning, and decays only when t is large enough.

6. Simulation results

In this paper, we use the *forward Euler method* to do the numerical simulations[8]. The corresponding finite difference schemes are:

$$\text{CFM:} \qquad Y_k^{(n)} = (I + M\Delta t)Y_k^{(n-1)} + \Delta t N Y_{k-1}^{(n-1)} \tag{26}$$

$$\text{BCM:} \qquad Y_k^{(n)} = (I + M\Delta t)Y_k^{(n-1)} + \Delta t N \frac{1}{2}\left(Y_{k-1}^{(n-1)} + Y_{k+1}^{(n-1)}\right) \tag{27}$$

where $Y_k^{(n)}$ is the state of cars k at time $n\Delta t$ and I is a 2×2 identity matrix. For small Δt (e.g. $\Delta t = 0.1$ second), the discrete simulation $Y_k^{(n)}$ approaches the result of the continuous function $Y_k(n\Delta t)$. If the initial states of all the cars are all zeros (i.e. $Y_k^{(0)} = \mathbf{0}$ for all k), and the state of the boundary (car 0) is also kept on as zeros (i.e. $Y_0^{(n)} = \mathbf{0}$ for all n), then the states of all the cars will be all zeros all the time. That is, the traffic system will maintain the equilibrium state shown Figure. 7. All the cars are spaced equally and move at the same speed.

If there is a small perturbation in the initial states $\mathbf{Y}^{(0)}$, the car-following system will become unstable quickly. Suppose that all the cars are spaced by 30 meters and moving at 90 km/h (i.e. 25 m/s) at the beginning. Let $k_d = 0.2$ (1/second), $k_v = 0.2$ (1/second^2) and $K =$

[8]Some more complicated schemes, e.g. the fourth order Runge-Kutta method, can also be used to solve the ODEs in (8) with much higher order accuracy. However, more memory space is need, and the computational cost is much higher. In real application, we want the implementation of the control system to be as simple as possible. Thus, in this paper, we use the forward Euler method for the numerical simulations.

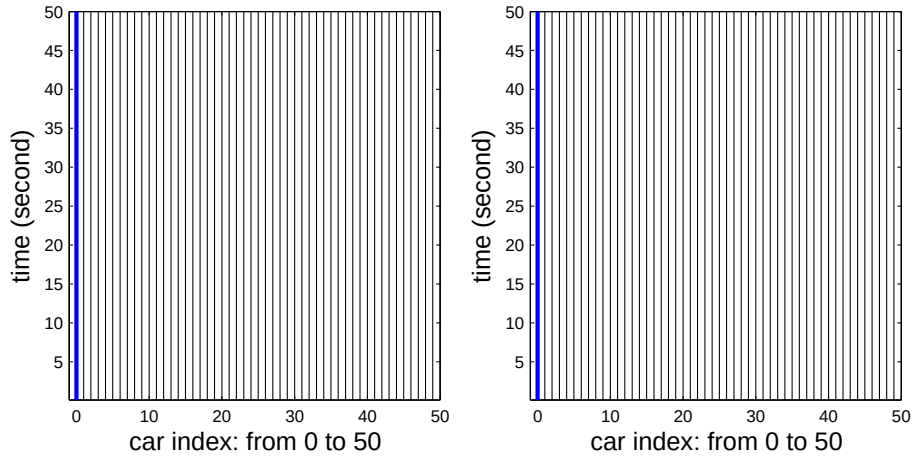

(a) $y_k(t)$ $(k = 1, 2, \cdots, 50)$ (b) $\dot{y}_k(t)$ $(k = 1, 2, \cdots, 50)$

Figure 7: If the traffic is stable, then all the cars will be spaced equally and move at the same speed. The relative position $y_k(t)$ and relative speed $\dot{y}_k(t)$ doesn't vary with time. Thus, $y_k(t)$ and $\dot{y}_k(t)$ are all vertical lines. The bold lines are the state of the first car (i.e. boundary).

50. Figure 8 shows the simulation result with small perturbations of the space between the cars, i.e. a random number in the range ± 1.5 m. The car-following system amplifies the small errors, and the traffic jam happens quickly. Moreover, the car-following model can not avoid collision. Bilateral control can suppress traffic instability effectively. The traffic system quickly becomes stable again, even if bilateral control is turned on only just before the traffic chaos caused by the car-following system sets in.

Figure 9 shows the simulation result with small perturbations of the relative speed of the cars, i.e. a random number in the range ± 1 m/s. The car-following model becomes unstable quickly and the traffic jam happens. Bilateral control suppresses traffic instability again. The bilateral control model is used just before the jam caused by the car-following model, and then the traffic system quickly becomes stable again.

Even if the initial condition is starting from the equilibrium state. Under car following control, the tiny small oscillation in the state of the first car (boundary) is amplified in the state of the second car, and then is amplified again in the state of the third car, and so on. Figure 10 shows the simulation result with small perturbations of the speed of the boundary car 0, i.e. a random number between ± 1 m/s. In the beginning, $y_k(0) = \dot{y}_k(0) = 0$ for all $k = 1, 2, \cdots, 50$. The car-traffic system under

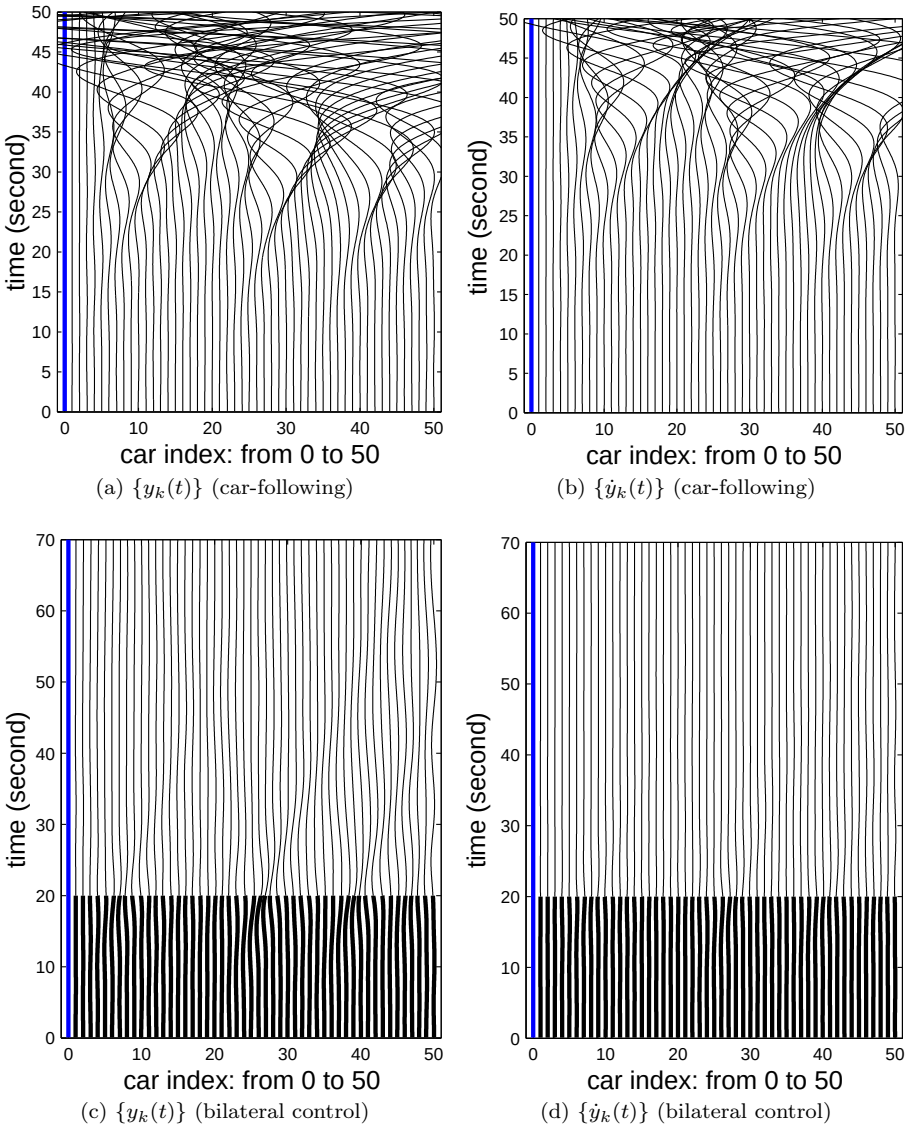

(a) $\{y_k(t)\}$ (car-following)

(b) $\{\dot{y}_k(t)\}$ (car-following)

(c) $\{y_k(t)\}$ (bilateral control)

(d) $\{\dot{y}_k(t)\}$ (bilateral control)

Figure 8: If there is small perturbations of the space between cars, then the car-following model will become unstable quickly (car collisions start at about 25 second). If bilateral control is used before collision, then the car-traffic system quickly becomes stable again. The first 20 seconds results in (c) and (d) are generated by car-following model, then bilateral control (fixed-free boundaries) is used promptly. The state of the first car (boundary) is set to be zero.

car-following control becomes unstable quickly. If bilateral control model is used in time, traffic instability can be suppressed efficiently.

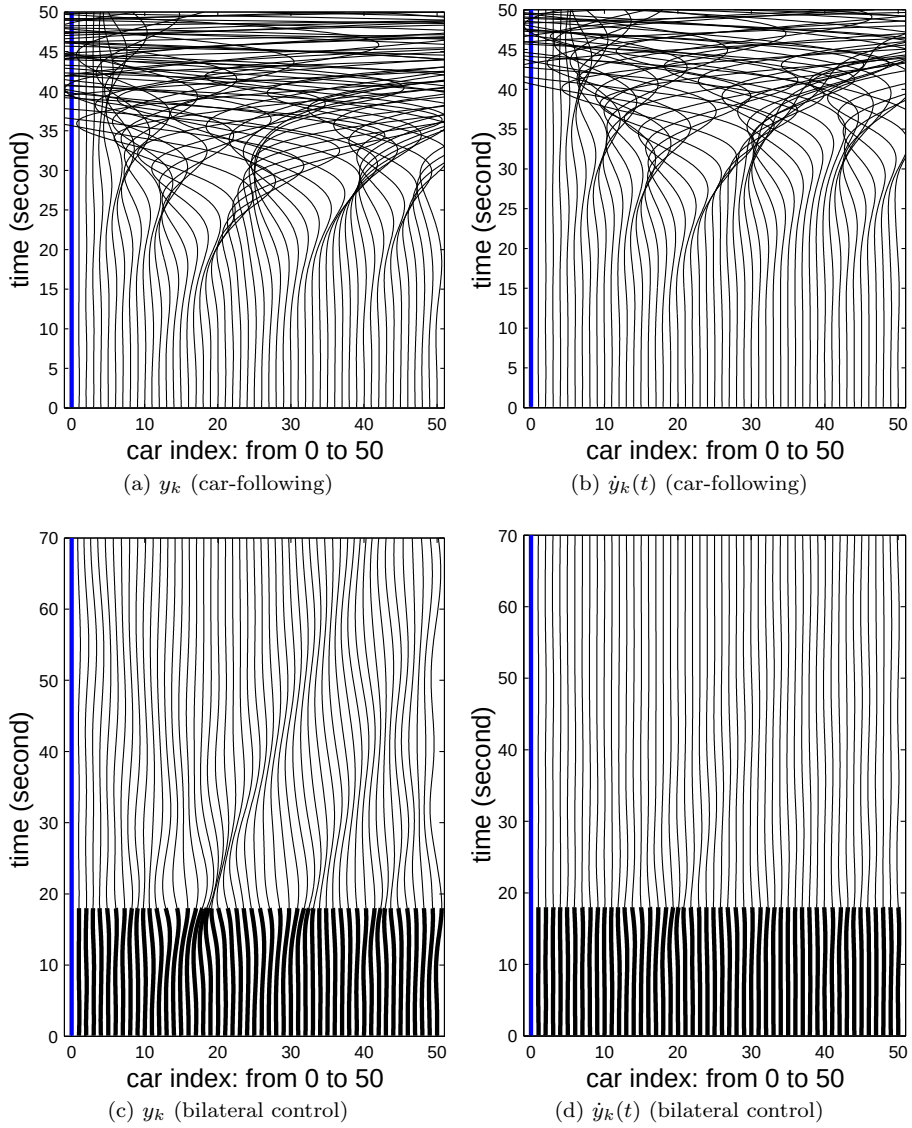

(a) y_k (car-following) (b) $\dot{y}_k(t)$ (car-following)

(c) y_k (bilateral control) (d) $\dot{y}_k(t)$ (bilateral control)

Figure 9: If there is small perturbation of the speed of the cars, then the car-following model will be unstable, and collision happens quickly (at about 22 second). If bilateral control is used before collision, then the car-traffic system becomes stable quickly. The first 18 seconds results in (c) and (d) are generated by car-following model, then bilateral control (fixed-free boundaries) is used promptly. The state of the first car (boundary) is set to be zero.

7. Conclusion

Bilateral control can suppress traffic instabilities. In this paper, we provide a theoretical analysis from the viewpoint of the eigenvalues and eigen-

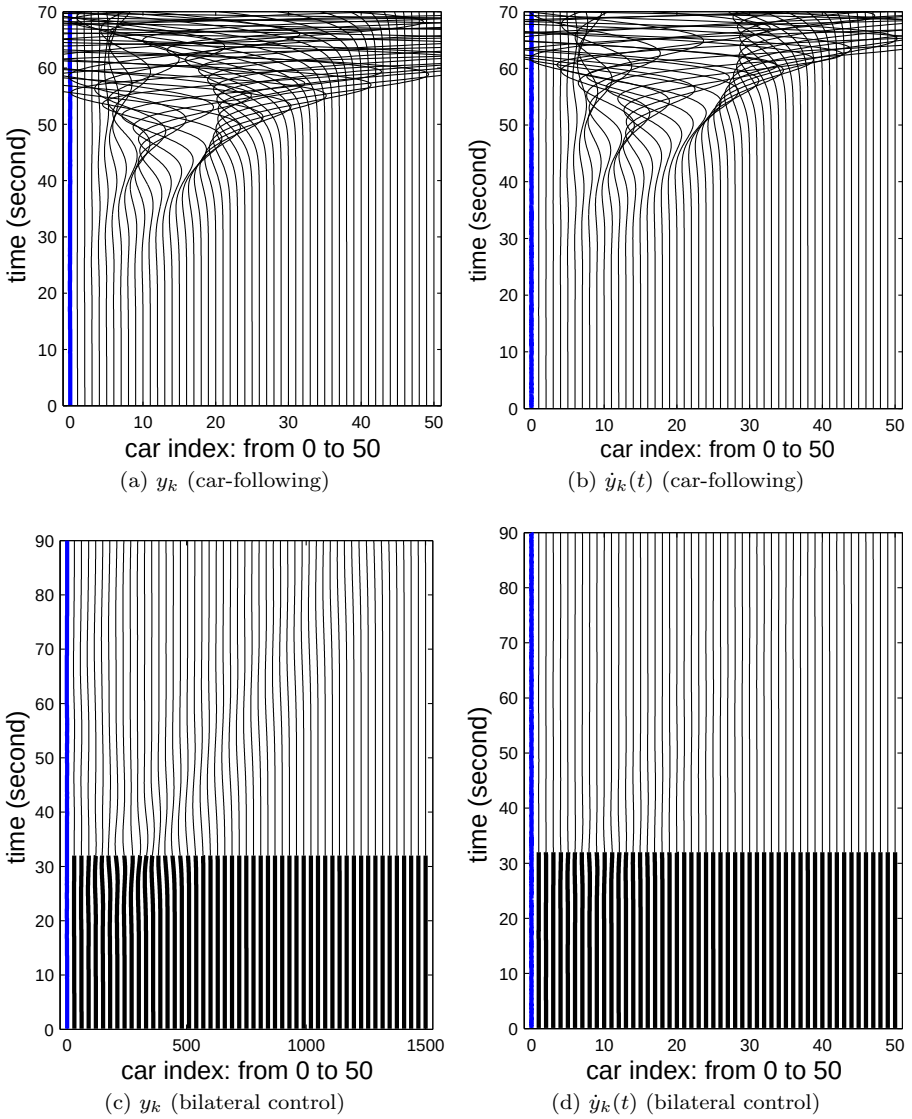

(a) y_k (car-following)

(b) $\dot{y}_k(t)$ (car-following)

(c) y_k (bilateral control)

(d) $\dot{y}_k(t)$ (bilateral control)

Figure 10: Under car following control, the tiny small oscillation in the state of the first (boundary) car is amplified in the state of the second car, and then is amplified again in the state of the third car, and so on. The collision happens quickly (at about 40 second). If bilateral control model is used before collision, e.g. at 32 second, then the car-traffic system becomes stable quickly. The initial condition is stating from the equilibrium state.

vectors of the corresponding linear system of ODEs. We show that the traditional car-following system is unstable because some eigenvalues of

the "big matrix" **A**, corresponding to its ODE system, have positive real parts. In contrast, the eigenvalues of the "big matrix" **B** corresponding to the ODE system for the bilateral control model all have non-positive real-part, thus, the traffic system will become stable from arbitrary initial state when using bilateral control. We also analyze the car-following model and bilateral control model under various boundary conditions.

"Don't tailgate." That is, don't come closer to the car in front of you than the distance that the car behind you is behind. This may be the big idea behind bilateral control. It is good for the community of drivers and provides advantages, such as freedom from traffic flow instabilities, which can be proven mathematically.

In this paper, we only considered the simplest models — the linear approximation of both the car-following system and bilateral control model. In real application, the speed of the car is limited to a range from $v_{\min}$ to $v_{\max}$, and the possible acceleration (and deceleration) of the car is also limited to some range from [$a_{\min}$ to $a_{\max}$. Moreover, k_d and k_v need not be constant, but can be chosen to be some functions of the relative distances and relative speeds. For example, the feedback gains k_d and k_v can be made inversely proportional to the distances and speed difference so as to provide stiffer control when neighboring cars are near. This appears to be what drivers actually do, mostly in order to avoid collisions in the car following situation.

In contrast, even the simplest linearized bilateral control model — with both k_d and k_v constants — can suppress traffic instabilities effectively. However, the bilateral control model can be improved beyond that simple linear version. For instance, both k_d and k_v in the bilateral control model can be made to be functions of the states of the neighboring cars to increase the safety margin, make the system more robust to sensor errors, increase fuel efficiency, of more aggressively damp traffic flow instabilities. Moreover, communication between cars can be used to further improve the safety margin and robustness of the system [15]. We plan to work on these aspects in future.

Appendix A. Stable condition of the car-following model

The two roots of eq. (12) are[9]:

$$\lambda(\omega) = -jk_v e^{-j\omega/2} \sin\left(\frac{\omega}{2}\right) \pm \sqrt{-e^{-j\omega} \sin^2\left(\frac{\omega}{2}\right) k_v^2 - 2jk_d e^{-j\omega/2} \sin\left(\frac{\omega}{2}\right)}$$

[9] In this paper, the square root of a complex number is chosen as the one with positive-real part. (In our case, the real part of the square root is not zero).

First, The real part of the sum of the two roots is smaller than zero,

$$c(\omega) = \Re\left\{-jk_v e^{-j\omega/2}\sin\left(\frac{\omega}{2}\right)\right\} = -k_v \sin^2\left(\frac{\omega}{2}\right) < 0 \tag{A.1}$$

Thus, one of the $\lambda(\omega)$ must be with non-positive real part. Furthermore, we can calculate

$$R(\omega) = \Re\left\{-e^{-j\omega}\sin^2\left(\frac{\omega}{2}\right)k_v^2 - 2jk_d e^{-j\omega/2}\sin\left(\frac{\omega}{2}\right)\right\} \tag{A.2}$$

$$= -\sin^2\left(\frac{\omega}{2}\right)\left[\left(1-2\sin^2\left(\frac{\omega}{2}\right)\right)k_v^2 + 2k_d\right] \tag{A.3}$$

$$I(\omega) = \Im\left\{-e^{-j\omega}\sin^2\left(\frac{\omega}{2}\right)k_v^2 - 2jk_d e^{-j\omega/2}\sin\left(\frac{\omega}{2}\right)\right\} \tag{A.4}$$

$$= 2\cos\left(\frac{\omega}{2}\right)\sin\left(\frac{\omega}{2}\right)\left[\sin^2\left(\frac{\omega}{2}\right)k_v^2 - k_d\right] \tag{A.5}$$

where $\Re\{f\}$ and $\Im\{f\}$ denote the real and imaginary part of the complex number f. Then we can calculate

$$\begin{aligned} d(\omega) &= \Re\left\{\sqrt{R(\omega)+jI(\omega)}\right\} \\ &= \pm\frac{1}{\sqrt{2}}\sqrt{R(\omega)+\sqrt{R^2(\omega)+I^2(\omega)}} \end{aligned}$$

For easy analysis, let $p = \sin^2(\omega/2)$. The condition of non-positive-real-part of $\lambda(\omega)$ is that the inequality $d^2(\omega) \le c^2(\omega)$ holds for all $0 \le p \le 1$, that is,

$$I^2(\omega) \le 4c^4(\omega) - 4c^2(\omega)R(\omega) \tag{A.6}$$

By tedious calculation, we can obtain the equivalent expression of eq.(A.6). That is, for all $0 \le p \le 1$

$$p\left(p - \frac{1}{2(k_v^2/k_d)+1}\right) \ge 0 \tag{A.7}$$

Eq.(A.7) implies that $k_v^2/kd \to \infty$. Note that k_v is a finite number (in general, $k_v < 1$). Thus, the condition $k_v^2/kd \to \infty$ means $k_d = 0$. That is, only the car's speed is used by the control system, and finally all cars move at the same speed. (Note that no guarantee of avoiding collision during this process.)

In the case of circular boundary condition, ω is sampled as K points $\{2\pi k/K\}$, and $p = \sin^2(\omega/2)$ is also sampled as K points:

$$p_k = \sin^2(k\pi/K), \qquad (k = 0, 1, 2, \cdots, K-1)$$

The corresponding equivalent condition of "non-positive real part for all eigenvalues" is that eq.(A.7) holds for p chosen as all of the K sampled points $\{p_k\}$. Note that $p_0 = 0$, the secondary smallest number is p_1.

Thus, all sample points $\{p_k\}$ will satisfy eq.(A.7) if and only if p_1 satisfies eq.(A.7). Now, we obtain the following condition for the stabilization of the "car-following" model:

$$\frac{1}{2(k_v^2/k_d)+1} \leq \sin^2(\pi/K) \tag{A.8}$$

that is,

$$\frac{k_v^2}{k_d} \geq \frac{1}{2}\left(\frac{1}{\sin^2(\pi/K)} - 1\right) \approx \frac{K^2}{2\pi^2} \tag{A.9}$$

As K increases, this condition will be more and more difficult to satisfy.

Appendix B. Similarity to the block Jordan form

For the car-following model with fixed boundary condition, the "big matrix" $\mathbf{A}$ is

$$\mathbf{A} = \begin{pmatrix} M & & & & \\ N & M & & & \\ & N & M & & \\ & & \ddots & \ddots & \\ & & & N & M \end{pmatrix}$$

where M and N are 2×2 matrices. We want to diagonalize both M and N by a *similarity transform*. Start with the eigenvalue-eigenvector decomposition of the 2×2 matrix M:

$$M = P\Lambda P^{-1} = P \begin{pmatrix} \lambda_1 & \\ & \lambda_2 \end{pmatrix} P^{-1}$$

Then all blocks M in $\mathbf{A}$ are changed to Λ by a simple similarity, and all blocks N are changed to $A = P^{-1}NP$:

$$\mathbf{S}^{-1}\mathbf{A}\mathbf{S} = \mathbf{F} \tag{B.10}$$

where

$$\mathbf{S} = \begin{pmatrix} P & & & & \\ & P & & & \\ & & P & & \\ & & & \ddots & \\ & & & & P \end{pmatrix}, \quad \mathbf{F} = \begin{pmatrix} \Lambda & & & & \\ A & \Lambda & & & \\ & A & \Lambda & & \\ & & \ddots & \ddots & \\ & & & A & \Lambda \end{pmatrix}$$

and

$$\Lambda = \begin{pmatrix} \lambda_1 & \\ & \lambda_2 \end{pmatrix}, \quad A = P^{-1}NP = \begin{pmatrix} a_{11} & a_{12} \\ a_{21} & a_{22} \end{pmatrix}$$

Now we want to change the 2×2 submatrices A to diagonal matrices D. This is achieved by a second similarity transform of the big matrix $\mathbf{F}$ using 2×2 blocks C:

$$\mathbf{FW} = \mathbf{WL} \tag{B.11}$$

where

$$\mathbf{W} = \begin{pmatrix} I & & & & \\ C & I & & & \\ & C & I & & \\ & & \ddots & \ddots & \\ & & & C & I \end{pmatrix}, \quad \mathbf{L} = \begin{pmatrix} \Lambda & & & & \\ D & \Lambda & & & \\ & D & \Lambda & & \\ & & \ddots & \ddots & \\ & & & D & \Lambda \end{pmatrix}$$

and

$$C = \begin{pmatrix} c_{11} & c_{22} \\ c_{21} & c_{22} \end{pmatrix}, \quad D = \begin{pmatrix} d_1 & \\ & d_2 \end{pmatrix}$$

Eq. (B.11) is equivalent to a *Sylvester equation* for C:

$$\Lambda C + A = D + C\Lambda, \quad \text{or} \quad C\Lambda - \Lambda C = A - D \tag{B.12}$$

Solutions C and D are not unique, but they exist. In fact only c_{12} and c_{21} are determined by eq. (B.12)

$$(\lambda_1 - \lambda_2) \begin{pmatrix} 0 & -c_{12} \\ c_{21} & 0 \end{pmatrix} = \begin{pmatrix} a_{11} - d_1 & a_{12} \\ a_{21} & a_{22} - d_2 \end{pmatrix}$$

The entries c_{11} and c_{22} are arbitrary and we choose $c_{11} = c_{22} = 0$. The diagonal matrix D and the matrix C are

$$D = \begin{pmatrix} a_{11} & \\ & a_{22} \end{pmatrix} \quad \text{and} \quad C = \frac{1}{\lambda_1 - \lambda_2} \begin{pmatrix} 0 & -a_{12} \\ a_{21} & 0 \end{pmatrix} \tag{B.13}$$

Now eq. (B.11) holds. The diagonal blocks I lead to determinant of $\mathbf{W}$ equal to 1, thus $\mathbf{W}$ is invertible and $\mathbf{F}$ is similar to $\mathbf{L}$.

Then the combined effect of the similarities in eq. (B.10) and (B.11) is to produce diagonal blocks Λ and D to replace M and N in the big matrix:

$$(\mathbf{SW})^{-1}\mathbf{A}(\mathbf{SW}) = \mathbf{L} \tag{B.14}$$

The exponentials $e^{t\mathbf{A}}$ show the fast growth of perturbations in the car-following system. Using this similarity, the same information is in $e^{t\mathbf{L}}$ — and it is simpler to analyze because Λ and D are diagonal.

From the matrix $\mathbf{L}$, it is a short step to the *official Jordan form* $\mathbf{J}$. Then $e^{t\mathbf{J}}$ has the same growth information as $e^{t\mathbf{L}}$. The Jordan form $\mathbf{J}$ has just 2 blocks with the eigenvalues λ_1 and λ_2 — each repeated K times

with only one eigenvector,

$$\mathbf{J} = \begin{pmatrix} J_1 & \\ & J_2 \end{pmatrix}$$

where J_1 and J_2 are both $K \times K$ *Jordan blocks*:

$$J_1 = \begin{pmatrix} \lambda_1 & & & & \\ 1 & \lambda_1 & & & \\ & 1 & \lambda_1 & & \\ & & \ddots & \ddots & \\ & & & 1 & \lambda_1 \end{pmatrix}, \quad J_2 = \begin{pmatrix} \lambda_2 & & & & \\ 1 & \lambda_2 & & & \\ & 1 & \lambda_2 & & \\ & & \ddots & \ddots & \\ & & & 1 & \lambda_2 \end{pmatrix}$$

First, $\mathbf{G}$ comes from $\mathbf{L}$ by a simple permutation of the rows and the same permutation of the columns:

- Rows (and columns) 1 to K of $\mathbf{G}$ come from rows (and columns) $1, 3, 5, \cdots, 2K-1$ of $\mathbf{L}$.
- Rows (and columns) $K+1$ to $2K$ of $\mathbf{G}$ come from rows (and columns) $2, 4, 6, \cdots, 2K$ of $\mathbf{L}$.

Thus, $\mathbf{G}$ is similar to $\mathbf{L}$:

$$\mathbf{G} = \mathbf{PLP}^{-1} = \mathbf{PLP}^T \tag{B.15}$$

The form of $\mathbf{G}$ is

$$\mathbf{G} = \begin{pmatrix} G_1 & \\ & G_2 \end{pmatrix}$$

where G_1 and G_2 are both $K \times K$ matrices:

$$G_1 = \begin{pmatrix} \lambda_1 & & & & \\ d_1 & \lambda_1 & & & \\ & d_1 & \lambda_1 & & \\ & & \ddots & \ddots & \\ & & & d_1 & \lambda_1 \end{pmatrix}, \quad G_2 = \begin{pmatrix} \lambda_2 & & & & \\ d_2 & \lambda_2 & & & \\ & d_2 & \lambda_2 & & \\ & & \ddots & \ddots & \\ & & & d_2 & \lambda_2 \end{pmatrix}$$

and the form of the *permutation matrix* $\mathbf{P}$ is

$$\mathbf{P} = \begin{pmatrix} P_1 \\ P_2 \end{pmatrix}$$

where P_1 and P_2 are both $K \times 2K$ matrices:

$$P_1 = \begin{pmatrix} 1 & 0 & 0 & 0 & 0 & 0 & 0 & \cdots & 0 & 0 \\ 0 & 0 & 1 & 0 & 0 & 0 & 0 & \cdots & 0 & 0 \\ 0 & 0 & 0 & 0 & 1 & 0 & 0 & \cdots & 0 & 0 \\ \vdots & \vdots & \vdots & \vdots & \vdots & \vdots & \vdots & \vdots & \vdots & \vdots \\ 0 & 0 & 0 & 0 & 0 & 0 & 0 & \cdots & 1 & 0 \end{pmatrix}$$

$$P_2 = \begin{pmatrix} 0 & 1 & 0 & 0 & 0 & 0 & 0 & \cdots & 0 & 0 \\ 0 & 0 & 0 & 1 & 0 & 0 & 0 & \cdots & 0 & 0 \\ 0 & 0 & 0 & 0 & 0 & 1 & 0 & \cdots & 0 & 0 \\ \vdots & \vdots & \vdots & \vdots & \vdots & \vdots & \vdots & \vdots & \vdots & \vdots \\ 0 & 0 & 0 & 0 & 0 & 0 & 0 & \cdots & 0 & 1 \end{pmatrix}$$

This permutation matrix $\mathbf{P}$ is famous for its use in the *fast Fourier transform* (FFT) algorithm [19].

A final similarity with a diagonal matrix $\mathbf{D}$ will replace d_1 and d_2 in $\mathbf{G}$ by 1 — to produce the official Jordan form of the car-following matrix $\mathbf{A}$. The form of the diagonal matrix $\mathbf{D}$ is

$$\mathbf{D} = \begin{pmatrix} D_1 & \\ & D_2 \end{pmatrix}$$

where D_1 and D_2 are both $K \times K$ diagonal matrices:

$$D_1 = \begin{pmatrix} d_1 & & & & \\ & d_1^2 & & & \\ & & d_1^3 & & \\ & & & \ddots & \\ & & & & d_1^K \end{pmatrix}, \quad D_2 = \begin{pmatrix} d_2 & & & & \\ & d_2^2 & & & \\ & & d_2^3 & & \\ & & & \ddots & \\ & & & & d_2^K \end{pmatrix}$$

We can check that

$$\mathbf{D}^{-1}\mathbf{G}\mathbf{D} = \mathbf{J} \tag{B.16}$$

Again, our purpose is to construct a matrix $\mathbf{J}$ similar to the original $\mathbf{A}$ with a convenient exponential:

$$\mathbf{A} = \mathbf{E}\mathbf{J}\mathbf{E}^{-1} \tag{B.17}$$

and $\mathbf{E} = \mathbf{S}\mathbf{W}\mathbf{P}^T\mathbf{D}$.

Appendix C. Car-following model with adaptive safe distance

In simple CFM (1) — also known as the "constant headway" control, the safe distance is a fixed number s. A more complicated model —

which is closer to human driver's behavior — is known as "constant time headway" control policy in leader following, in which the safe distance is chosen adaptively according to the car's speed:

$$s_i = v_i T \tag{C.18}$$

where T is known as the response time, that is, the time taken by the current car to react to sudden braking of the leading car[10]. In general, T is chosen to be about one second. Now, the simple CFM (1) becomes:

$$a_i = k_d(x_{i-1} - x_i) + k_v(v_{i-1} - (1+\tau)v_i) \tag{C.19}$$

where $\tau = Tk_d/k_v$ is positive. The eigenvalue-eigenvector decomposition method still works for analyzing this new car-following model (C.19) with adaptive safe distance. Only a small modification is needed. First, let $s = 0$ in (3), and then let the 2×2 matrix M be

$$M = \begin{pmatrix} 0 & 1 \\ -k_d & -(1+\tau)k_v \end{pmatrix}$$

We can build the same "big ODE" system as in (8). The eigenvalues of the block-Toeplitz matrix $\mathbf{A}$ are the roots of the following characteristic equation (see eq. (12))

$$\lambda^2(\omega) + \big(1 - w(\omega) + \tau\big)k_v\lambda(\omega) + \big(1 - w(\omega)\big)k_d = 0 \tag{C.20}$$

where $w(\omega) = e^{-j\omega}$. The $c(\omega)$ in (A.1) becomes

$$c(\omega) = -k_v \sin^2\left(\frac{\omega}{2}\right) - \frac{\tau}{2}k_v < 0$$

and the $R(\omega)$ in (A.3) and $I(\omega)$ in (A.5) become

$$R(\omega) = -\sin^2\left(\frac{\omega}{2}\right)\left[\left(1 - \tau - 2\sin^2\left(\frac{\omega}{2}\right)\right)k_v^2 + 2k_d\right] + \frac{\tau^2}{4}k_v^2$$
$$I(\omega) = 2\cos\left(\frac{\omega}{2}\right)\sin\left(\frac{\omega}{2}\right)\left[\sin^2\left(\frac{\omega}{2}\right)k_v^2 - k_d + \frac{\tau}{2}k_v^2\right]$$

correspondingly. The stability condition (A.7) gives the following constraint:

$$p\left(p - \frac{1 - (\tau^2/2 + \tau)(k_v^2/k_d)}{2(k_v^2/k_d) + 1 + \tau k_v^2/k_d}\right) \geq 0 \tag{C.21}$$

where $p = \sin^2(\omega/2)$ is in the range from 0 to 1. Thus, the stability condition is

$$1 - (\tau^2/2 + \tau)(k_v^2/k_d) \leq 0$$

[10] A more detailed analysis takes into account possible differences in the speeds of the vehicles as well.

Or (by substituting $\tau = Tk_d/k_v$)

$$k_d T^2 + 2k_v T - 2 \geq 0$$

That is

$$T \geq \frac{\sqrt{2k_d + k_v^2} - k_v}{k_d} \tag{C.22}$$

Comparing this with the original "constant headway" control (1) — whose stability condition (A.7) can *not* be satisfied — we note that the stability condition (C.21) of the "constant time headway" control (C.19) can be satisfied under certain conditions. However, the (equivalent) stability condition (C.22) is still difficult to satisfy in a real traffic system. For instance, when both k_d and k_v are in the (reasonable) range from 0 to 0.2, the "response time" T must be larger than 2.3166 seconds (that minimum for T occurs when $k_d = 0.2$ and $k_v = 0.2$). We get a value close to 1 second for T only when both k_d and k_v are larger than 0.66.

Note that the stability condition (C.22) provides a critical limitation on the traffic throughput[11]. If the traffic throughput is larger than $k_d/(\sqrt{2k_d + k_v^2} - k_v)$ (see eq. (C.22)), then traffic flow instabilities will arise (or collisions will result). This corresponds to our experience that at low densities there may be few problems, but that at high densities flow instabilities ("phantom traffic jams") will occur.

References

1. B. K. Horn, Suppressing traffic flow instabilities, 16th International IEEE Conference on Intelligent Transportation Systems (ITSC 2013), IEEE, 2013 pp. 13–20.
2. H. Greenberg, An analysis of traffic flow, *Operations research* 7:79–85 (1959).
3. R. E. Chandler, R. Herman, and E. W. Montroll, Traffic dynamics: studies in car following, *Operations research* 6:165–184 (1958).
4. R. Herman, E. W. Montroll, R. B. Potts, and R. W. Rothery, Traffic dynamics: analysis of stability in car following, *Operations research* 7:86–106 (1959).
5. L. C. Edie, Car-following and steady-state theory for noncongested traffic, *Operations Research* 9:66–76 (1961).
6. P. I. Richards, Shock waves on the highway, *Operations research* 4:42–51 (1956).
7. T. Nagatani, Traffic jams induced by fluctuation of a leading car, *Physical Review E* 61:3534 (2000).
8. W. S. Levine and M. Athans, On the optimal error regulation of a string of moving vehicles, *IEEE Transactions on Automatic Control* (1966).
9. D. N. Godbole and J. Lygeros, Longitudinal control of the lead car of a platoon, *IEEE Transactions on Vehicular Technology* 43:1125–1135 (1994).

[11] The traffic throughput is defined as $v/(l + vT)$ (which is less than $1/T$), where v is the car's speed and l is the car length.

10. C. Chien, Y. Zhang, and C. Cheng, Autonomous intelligent cruise control using both front and back information for tight vehicle following maneuvers, American Control Conference, Proceedings of the 1995, vol. 5 IEEE, 1995 pp. 3091–3095.
11. P. Barooah, P. G. Mehta, and J. P. Hespanha, Mistuning-based control design to improve closed-loop stability margin of vehicular platoons, *IEEE Transactions on Automatic Control* 54:2100–2113 (2009).
12. F. Lin, M. Fardad, and M. R. Jovanovic, Optimal control of vehicular formations with nearest neighbor interactions, *IEEE Transactions on Automatic Control* 57:2203–2218 (2012).
13. M. R. Jovanovic and B. Bamieh, On the ill-posedness of certain vehicular platoon control problems, *IEEE Transactions on Automatic Control* 50:1307–1321 (2005).
14. B. Bamieh, M. R. Jovanovic, P. Mitra, and S. Patterson, Coherence in large-scale networks: Dimension-dependent limitations of local feedback, *IEEE Transactions on Automatic Control* 57:2235–2249 (2012).
15. T. A. Baran and B. K. Horn, A robust signal-flow architecture for cooperative vehicle density control., ICASSP, 2013 pp. 2790–2794.
16. A. Nakayama, Y. Sugiyama, and K. Hasebe, Effect of looking at the car that follows in an optimal velocity model of traffic flow, *Physical Review E* 65:016112 (2001).
17. M. Treiber and D. Helbing, Hamilton-like statistics in onedimensional driven dissipative many-particle systems, *The European Physical Journal B* 68:607–618 (2009).
18. G. Strang, *Introduction to linear algebra*, Wellesley-Cambridge Press, 2016.
19. G. Strang, *Computational science and engineering*, Wellesley-Cambridge Press, 2007.

CSAIL, MIT, Cambridge, USA, 02139

Department of Mathematics, MIT, Cambridge, USA, 02139